

Article

Extending and Solving the Refrigerated Routing Problem

Sara Ceschia ^{*,†}, Luca Di Gaspero [†] and Antonella Meneghetti [†]

DPIA—Polytechnic Department of Engineering and Architecture, University of Udine, Via delle Scienze 206, 33100 Udine, Italy; luca.digaspero@uniud.it (L.D.G.); antonella.meneghetti@uniud.it (A.M.)

* Correspondence: sara.ceschia@uniud.it

† All the authors contributed equally to this work.

Received: 15 September 2020; Accepted: 20 November 2020; Published: 26 November 2020



Abstract: In recent years, cold food chains have shown an impressive growth, mainly due to customers life style changes. Consequently, the transportation of refrigerated food is becoming a crucial aspect of the chain, aiming at ensuring efficiency and sustainability of the process while keeping a high level of product quality. The recently defined Refrigerated Routing Problem (RRP) consists of finding the optimal delivery tour that minimises the fuel consumption for both the traction and the refrigeration components. The total fuel consumption is related, in a complex way, to the distance travelled, the vehicle load and speed, and the outdoor temperature. All these factors depend, in turn, on the traffic and the climate conditions of the region where deliveries take place and they change during the day and the year. The original RRP has been extended to take into account also the total driving cost and to add the possibility to slow down the deliveries by allowing arbitrarily long waiting times when this is beneficial for the objective function. The new RRP is formulated and solved as both a Mixed Integer Programming and a novel Constraint Programming model. Moreover, a Local Search metaheuristic technique (namely Late Acceptance Hill Climbing), based on a combination of different neighborhood structures, is also proposed. The results obtained by the different solution methods on a set of benchmarks scenarios are compared and discussed.

Keywords: energy efficiency; sustainable transports; cold food chain; rich vehicle routing problem; mixed integer programming; constraint programming; local search

1. Introduction

In the last decade, cold chains have recorded an impressive growth due to both urbanization and lifestyle changes, which have produced an increasing demand of ready-to-use refrigerated and frozen food. In the near future, the global refrigerated transport market is projected to reach USD 21.6 billion by 2025 at CAGR (Compound Annual Growth Rate) of 5.8 %, with the frozen food segment recording the fastest growth [1].

However, the transport sector is known to be one of the major contributor to global energy consumption and related greenhouse gas (GHG) emissions. Therefore, the transition towards sustainable transport, which can be defined as a way of the transport sector to embrace the concept of sustainable development, has attracted great attention of academics, industry practitioners and governments in the last two decades, as highlighted in the recent review by Zhao et al. [2].

In the cold chain, sustainability has an even greater role due to additional energy required to assure the proper control of food temperature [3]. Since a temperature raise might be harmful for both the safety and the quality of the delivered products, the refrigeration needs adds additional energy requirements to vehicle traction, thus increasing fuel consumption and greenhouse GHG emissions. Indeed, increasing the efficiency of refrigerated transport is ranked as the third energy

saving potential among cold chain processes (James et al. [4]). Furthermore, even if the cold chain logistics market is prosperous, cold chain logistics companies are usually small in scale and numerous in quantity, thus leading to high costs and high carbon emissions during transportation [5]. Therefore, reducing the total delivery cost and energy consumption becomes crucial to guide the transition towards sustainable transports and making cold chain logistics companies both competitive and compliant to environment preservation.

The problem of planning the route for a refrigerated vehicle (Refrigerated Routing Problem, RRP) has received attention only recently [6]. Differently from traditional routing problems, both the traction and refrigeration fuel consumption should be taken into account [7]. The latter depend on the outdoor temperature, which varies along a day and also in the different seasons of a year, so that a multi-period model has to be considered. The route with minimum total fuel consumption will be selected depending on both the delivery tour and the hourly profile of temperature along a year of the specific region where the delivery tour takes place.

In order to better embrace the sustainable transport concept both in its economic and environmental dimensions, the routing problem for a refrigerated vehicle should take into account also the driver wage policy, since the driver wage is a relevant component of travel costs as underlined by Stellingwerf et al. [7]. However, the multi-period modelling proposed in [6] should be preserved in order to better estimate fuel consumption during a real delivery process. Furthermore, to adhere to typical drivers' behaviour, which is prone to avoid traffic congestion, arbitrary waiting times at clients should be allowed, slowing down the delivery plan if it turns out to be beneficial for the overall cost function, which involves both the fuel cost for refrigeration and traction and the wage cost. Since the latter is assumed proportional to the delivery duration in most routing literature (see also the recent JRC (Research Centre of the European Commission) Report on road transports costs in Europe [8]), then the opportunity of delaying departure from clients should be investigated.

Therefore, in this paper a new formulation of the RRP is provided, by introducing the wage cost and arbitrary waiting times to complete the delivery tour, taking into account the hourly profile of temperature of the region along the year, as well as hourly speed pattern due to congestion. A new mathematical formulation is proposed in terms of both a Mixed Integer Programming (MIP) model and a novel Constraint Programming (CP) model. A metaheuristic solution technique based on the Local Search paradigm, which uses a composition of two neighborhood relations, is also provided in order to solve larger test cases in shorter computational time. Two datasets of instances have been generated by means of a parametrised instance generator that uses real data about climate conditions and travel times. The proposed solution methods are compared on benchmark instances, both in terms of solution quality and running times. All instances, along with our best solutions, have been made available on the web to encourage future comparisons.

The remainder of the paper is organised as follows. Section 2 presents an overview of the literature about sustainable routing problems. The extended RRP is formally described in Section 3 along with the MIP model, while the CP model and the LS metaheuristic are presented in Section 4. Section 5 reports results. In particular, the reference scenario is described in Section 5.1, while the solution methods are empirically compared in Section 5.2, which reports the outcomes of the computational experiments. The analysis of cost and energy performance for the basic reference scenario are reported in Section 5.3 and in Section 5.4 a further performance analysis on a traffic-congested scenario is provided. Section 5.5 reports the sensitivity analysis on the driver wage costs, whereas Section 5.6 discusses the adoption of different policies for the driver wage cost. Finally, some conclusions are derived in Section 6.

2. Sustainable Routing: A Literature Overview

The growing attention to sustainability issues in logistics has attracted the interest of the research community that introduced the concept of Green Logistics [9]. The class of Green Vehicle Routing

Problems (GVRP), in particular, is characterised by the commitment of balancing the environmental and economic costs by implementing effective vehicle routes and schedules.

In this context, the Pollution Routing Problem (PRP) was firstly presented by Bektaş and Laporte [10] as a variant of the classical Capacitated Vehicle Routing Problem, in which the goal is to minimise a more comprehensive objective function that accounts for GHG emissions, fuel consumption, and driver costs. The authors proposed different mathematical models and reported computational experiments on realistic instances up to 20 nodes. For the solution of the PRP, Demir et al. [11] devised an Adaptive Large Neighborhood Search (ALNS) heuristic combined with a speed optimisation procedure. The same authors improved and adapted the ALNS algorithm to solve a Bi-Objective PRP [12], where the fuel consumption and driving time objective are considered separately.

Franceschetti et al. [13] tackled the PRP with traffic congestion (Time-Dependent PRP) by considering a two-level speed function: the peak-period, when the vehicle must travel at a congestion speed, and the following period, when the vehicle runs at free flow speed, respecting legal limits only. They provided an Integer Linear Programming formulation (ILP) for this problem and investigated in which cases the travel costs can be reduced by allowing vehicles to wait at nodes, depending on driver wage policies and modelling traffic congestion. In a subsequent work, Franceschetti et al. [14] presented an ALNS heuristic for the solution of the Time-Dependent PRP with several insertion and removal operators specifically tailored to the problem with traffic congestion. While in the Time-Dependent PRP the free flow speed is optimised, Ehmke et al. [15,16] studied the problem of routing a fleet of vehicles minimising gas emissions in urban areas, where vehicles travel at speed of traffic and no waiting time is allowed at customer locations. A detailed sensitivity analysis is performed on real-world and generated test instances, analysing varying geographies, departure times, demand quantities and vehicle types.

The problem of modeling time-varying traffic conditions has been widely discussed also by Xiao and Konak [17] in the context of GVRP. The GVRP proposed by Xu et al. [18] considers a non-linear time-varying vehicle speed and soft time windows. The problem is formulated as a Mixed Integer Non-Linear Programming model and solved by a Genetic Algorithm embedding adaptive greedy strategies. Xiao et al. [19] proposed a fuel consumption optimisation model for the Capacitated Vehicle Routing Problem, where the objective function depends both on the distance travelled and the carried load. As a solution technique, they implemented a Simulated Annealing algorithm which uses a combination of three neighborhood structures (Swap, Relocation and 2-Opt). A further extension to the PRP has been proposed by Koç et al. [20], who introduced the Fleet Size and Mix PRP where a heterogenous fleet of vehicles is considered. The problem is solved by means of a hybrid evolutionary metaheuristic and extensive computational experiments on realistic and artificial instances demonstrated the benefits of using a heterogenous fleet over a homogenous one.

Besides the specific domain of road logistics, there are other attempts to investigate the application of metaheuristic optimisation methods for sustainability in the context of maritime transportations. Among others, De et al. [21] studied sustainability aspects in the context of maritime transportation by considering a model that employs a non-linear fuel consumption function depending on the speed of the vessel and solve it through a Particle Swarm Optimisation algorithm. In [22], the authors deal with the more complex problem of the definition of strategies for the optimisation, in a sustainability perspective, of fuel bunker management and their impact in container shipping operation, in particular considering disruption and recovery policies.

Coming back to road logistics, the literature about transportation for cold chains is rather limited and focused mainly at supply chain level (e.g., [23–27]). At operational level, Hsu et al. [28] investigated the vehicle routing problem for the delivery of perishable food from a distribution center by considering loss of food during transport, energy consumed by storage equipment due to a fixed difference between indoor and outdoor temperature, and time-window constraints. Novaes et al. [29] introduced the Process Capability Indices (PCI) based on simulations of thermal characteristic of potential journeys

and product thermal properties in order to identify the route with the minimum travel distance, while respecting a minimum PCI value.

Meneghetti and Ceschia [6] addressed the routing problem of a refrigerated vehicle for palletized frozen food by defining the Refrigerated Routing Problem (RRP). The objective is to find the route with minimum fuel consumption, taking into account thermal loads depending on outdoor temperature, service times at each client based on the quantity to be unloaded, as well as different speeds depending on the hourly traffic situation. In this setting, traction and refrigeration requirements can vary throughout the day and also the different seasons of the year, so a multi-period model was developed. For the refrigeration load, in particular, the transmission and the infiltration components were considered, while the traction fuel requirements were modeled following the CMEM approach, dividing them into the weight, engine and speed module [14]. The problem was formulated by a Constraint Programming extended vehicle routing model and solved thorough the Gecode solver available in the MiniZinc suite [30]. Real-world test scenarios came from a company that supplies frozen bread dough to a local network of supermarkets. In addition, a sensitivity analysis on typical tour attributes such as customers' demand, start time of the delivery tour, seasonality, network complexity, and different climate conditions was performed.

Stellingwerf et al. [7] propose an extension of the GVRP model whose objective is to minimise emissions in temperature-controlled transportation systems. Similarly to Meneghetti and Ceschia [6], the objective function takes into account the fuel consumption for motive energy and for thermal energy and refrigerant leakage; in addition, the authors consider also the wage costs and a limit on the maximum driving time. Differently from Meneghetti and Ceschia [6], the model is not multi-period, such that a single value (30 °C) is considered for the outdoor temperature independently from the hour the day and the month of the year. In addition, it does not considered traffic condition varying during the day (speed values are fixed for each arc). The model is tested on a case study regarding the distribution of frozen food from a central distribution center to nine supermarkets in Netherlands.

This work aims to fill the gaps in existing literature by extending the model proposed in [6], embedding also the cost due to drivers, and proposing and comparing new solution approaches on different test cases.

3. Problem Description and Formulation

In the following, a detailed description and a mathematical formulation of the problem are proposed. The formulation is expressed in terms of a Mixed Integer Problem.

Let $\mathcal{G} = (\mathcal{N}, \mathcal{A})$ be a graph where $\mathcal{N} = \{0, \dots, n, n + 1\}$ is the set of nodes and \mathcal{A} is the set of arcs. The customers correspond to the nodes $\mathcal{C} = \{1, \dots, n\}$, whereas the starting depot is identified by the vertex 0 and the ending depot by $n + 1$ (usually they coincide, however, for more generality, it is convenient to consider them separately for an easier formulation). There are no arcs ending at vertex 0 or originating from vertex $n + 1$, but the subgraph induced by the set of customer nodes \mathcal{C} , is a complete graph. The distance between two nodes i and j is denoted by d_{ij} and it is expressed in kilometres.

Each customer $i \in \mathcal{C}$ has a non-negative demand q_i of palletized units, each of them having the weight μ . We denote with $Q = \sum_{i \in \mathcal{C}} q_i$ the total quantity requested, and by $D = \mu Q$ the total demand. In addition, we assume that the total demand D is always less or equal than the total vehicle capacity, so that all the customers can be served by just a single vehicle.

In order to deal with the real situation faced by the vehicle during the different times of the day we represent the variation of traveling speed during the day by means of a discrete function in the following way: there are $|S|$ time intervals $[\bar{t}_s^{min}, \bar{t}_s^{max})$, each one corresponding to a traffic time slot $s \in S$ and to a speed level \bar{v}^s .

On the basis of the previous input data, the main decision variables of the problem are x_{ij} , which assume value 1 if the arc (i, j) is included in the route and 0 otherwise (where $i \neq j, i \neq n + 1, j \neq 0$). We also introduce a set of integer decision variables $u_{ij} \geq 0$ that

represent the load of the vehicle on arc (i, j) and the set of binary variables z_{ij}^s that take value 1 if the arc (i, j) is traversed during timeslot $s \in S$ corresponding to speed level \bar{v}^s . Moreover, $t_i \geq 0$ represents the arrival time at customer i and s_i its service duration (both in seconds), whereas the binary variables w_{ij}^k are equal to 1 if the temperature slot (i.e., the time window) k is active on arc (i, j) (where K is the set of temperature slots in a day). Finally, r_{ij} are binary variables that assume value 1 if the first pallet of customer i to be unloaded is in the j -th position in the vehicle.

We adopt the fuel consumption non-linear formulation proposed in [6]. In the following we provide the details of the formulation, but we refer the interested reader to that paper for the detailed explanation of how it is derived. The objective function (Equation (1)) accounts for the total fuel consumption as the aggregation of three main components: the traction fuel consumption (F_{trac}), which according to the CMEM model [31] is in turn the sum of three modules (weight, engine and speed), the refrigeration fuel consumption (F_{refr}), which can also be further decomposed into transmission and infiltration consumption, and the driver wage (F_{driver}), which is the product of the driver cost by the total delivery time (travel and stops).

$$\min z = f_f \times F_{\text{trac}} + f_f \times F_{\text{refr}} + F_{\text{driver}} \quad [€] \tag{1}$$

$$F_{\text{driver}} = f_d \times v \times (t_{n+1} - t_0) \quad [€] \tag{2}$$

In Equation (2), given that the RRP is a multi-period problem, we aggregate the driver costs along the whole planning horizon, so that the single-route value has to be multiplied by the total number of delivery tours v .

The traction fuel consumption F_{trac} component is modelled in Equation (3), where α , β , and γ are parameters depending on the vehicle specifications reported in Table 1. The first term in Equation (3) corresponds to the weight module, since it depends on the curb weigh \bar{w} and the load u_{ij} carried by the vehicle on this arc; the second term is known as the engine module and it is linear on travel time; the third term is the speed module which grows with the square of the vehicle speed. Similarly to Equation (2), the single tour traction fuel consumption is multiplied by the total number of delivery tours v .

$$F_{\text{trac}} = v \times \left(\sum_{(i,j) \in \mathcal{A}} \alpha \times d_{ij} \times (\bar{w} \times x_{ij} + u_{ij}) + \sum_{(i,j) \in \mathcal{A}} \beta \times d_{ij} \times \sum_{s \in S} \frac{z_{ij}^s}{\bar{v}^s} + \sum_{(i,j) \in \mathcal{A}} \gamma \times d_{ij} \sum_{s \in S} z_{ij}^s (\bar{v}^s)^2 \right) \quad [l] \tag{3}$$

Table 1. Main input parameters.

Description	Value	Description	Value
α Weight module const.	$1.494 \times 10^{-5} \frac{1}{\text{kg km}}$	ϕ Fix time at customer	300 s
β Engine module const.	$5.54 \frac{1}{\text{h}}$	μ Palletized unit load	600 kg
γ Speed module const.	$3.962 \times 10^{-5} \frac{1 \text{h}^2}{\text{km}^3}$	δ Time to open/close doors	12 s
ζ Exchange surface	150 m^2	χ Movement time of forklift	36 s
v Global heat transfer coeff.	$0.44 \frac{\text{W}}{\text{m}^2 \text{K}}$	ψ Movement time in a row	3 s
\bar{w} Weight of empty vehicle	7450 kg	ϵ Units per row	3
σ Specific fuel consumption	$0.30 \frac{1}{\text{kWh}}$	f_d Driver cost	$0.0022 \frac{€}{\text{s}}$
f_f Fuel cost	$1.4 \frac{€}{\text{l}}$	T^{max} Max tour duration	9 h
ϑ Indoor temperature	$-20 \text{ } ^\circ\text{C}$	v Number of yearly tours	329

Constraints (4) and (5) impose that each customer must be visited exactly once in a route.

$$\sum_{j \in \mathcal{N} \setminus \{0, j \neq i\}} x_{ij} = 1 \quad \forall i \in \mathcal{N} \setminus \{n+1\} \tag{4}$$

$$\sum_{i \in \mathcal{N} \setminus \{n+1\}, j \neq i} x_{ij} = 1 \quad \forall j \in \mathcal{N} \setminus 0 \tag{5}$$

Constraints (6) and (7) force the load of the vehicle at the depot: the vehicle is fully loaded when the tour starts and empty when it returns to the depot.

$$\sum_{j \in \mathcal{C}} u_{0j} = D \tag{6}$$

$$\sum_{i \in \mathcal{C}} u_{i,n+1} = 0 \tag{7}$$

Constraints (8) and (9) set the vehicle load for the other arcs of the graph.

$$\sum_{j \in \mathcal{N} \setminus \{n+1\}} u_{ji} - \sum_{j \in \mathcal{N} \setminus 0} u_{ij} = \mu \times q_i \quad \forall i \in \mathcal{C} \tag{8}$$

$$x_{ij} \times (\mu \times q_j) \leq u_{ij} \leq x_{ij} \times (D - \mu \times q_i) \quad \forall (i, j) \in \mathcal{A} \tag{9}$$

Constraints (10) establish that exactly one speed level must be assigned to each arc of the route.

$$\sum_{s \in \mathcal{S}} z_{ij}^s = x_{ij} \quad \forall (i, j) \in \mathcal{A} \tag{10}$$

Constraints (11) and (12) define the relation between t_i and z_{ij}^s variables: if the vehicle departs from node i within the time interval $[\bar{t}_s^{min}, \bar{t}_s^{max})$, the z_{ij}^s is activated and the vehicle will travel at speed level \bar{v}^s on arc (ij) .

$$t_i + s_i \geq \sum_{s \in \mathcal{S}} \bar{t}_s^{min} \sum_j z_{ij}^s \quad \forall i \in \mathcal{N} \setminus \{n+1\} \tag{11}$$

$$t_i + s_i < \sum_{s \in \mathcal{S}} \bar{t}_s^{max} \sum_j z_{ij}^s \quad \forall i \in \mathcal{N} \setminus \{n+1\} \tag{12}$$

The refrigeration fuel consumption is reported in Equation (13). It depends on both the transmission and infiltration energy, which are affected by the outdoor temperature. The variation of the temperature during each day of the horizon is modelled similarly to the speed function with $|K|$ time slots $[\bar{\tau}_k^{min}, \bar{\tau}_k^{max})$ in a day.

Since the outdoor temperature within the same hour of the day varies seasonally, we consider $m \in M$ months in the planning horizon. Therefore, for each day timeslot k and each month of the horizon m , there are several corresponding parameter values: an outdoor temperature level $\bar{\theta}^{m,k}$, a specific coefficient of performance $\bar{\rho}^{m,k}$, an infiltration energy value $\bar{r}^{m,k}$, an infiltration power value $\bar{\zeta}^{m,k}$, and a number of occurrences $\bar{\eta}^{m,k}$ during the horizon.

$$F_{refr} = \sum_{(i,j) \in \mathcal{A}} (E_{ij}^{trans} + E_{ij}^{inf}) / \sigma \tag{13}$$

$$E_{ij}^{trans} = (t_j - t_i) \times \sum_{m \in M} \sum_{k \in K} \left(\bar{\eta}^m w_{ij}^k \times \frac{\bar{\zeta} \times v \times (\bar{\theta}^{m \cdot |K| + k} - \theta)}{\bar{\rho}^{m \cdot |K| + k}} \right) \tag{14}$$

According to [32], the infiltration power converges to a value $\bar{\zeta}^{m,k}$ 40 s after the doors have been opened. Consequently, the infiltration energy when the doors remain open for more than 40 s (which is the usual case when palletized units have to be removed) can be modelled as in Equation (15), where $\bar{r}^{m,k}$ is the infiltration contribution of the first 40 s.

$$E_{ij}^{inf} = \sum_{m \in M} \sum_{k \in K} \left(\bar{\eta}^m w_{ij}^k \times \frac{\bar{r}^{m \cdot |K| + k} + \bar{\zeta}^{m \cdot |K| + k} \times (s_i - 40)}{\bar{\rho}^{m \cdot |K| + k}} \right) \tag{15}$$

Notice that $\bar{\eta}^m$ is the number of working days of month m , while $l^{m,k}$, $\zeta^{m,k}$, and $\bar{\rho}^{m,k}$ are the specific parameter values of the time slot k of month m (e.g., 9:00–10:00, May). Constraints (16) and (17) define the relation between t_i and w_{ij}^k variables.

$$t_i \geq \sum_{k \in K} \bar{\tau}_k^{min} \sum_j w_{ij}^k \quad \forall i \in \mathcal{N} \setminus \{n+1\} \tag{16}$$

$$t_i < \sum_{k \in K} \bar{\tau}_k^{max} \sum_j w_{ij}^k \quad \forall i \in \mathcal{N} \setminus \{n+1\} \tag{17}$$

Constraints (18) establish that exactly one outdoor temperature time slot must be selected for each arc of the route.

$$\sum_{k \in K} w_{ij}^k = x_{ij} \quad \forall (i, j) \in \mathcal{A} \tag{18}$$

The service duration s_i is the time needed for unloading operations, which depends on the position of each palletized unit in the vehicle (for the depot the service duration is null), which can be estimated as in Equation (19).

$$s_i = \phi + 2 \times \delta + \sum_j^{Q-q_i} r_{ij} \sum_k^{q_i} \bar{r}_{j+k} \quad \forall i \in \mathcal{C} \tag{19}$$

For each customer i , the binary variable r_{ij} is positive if the first palletized unit to be unloaded is in the j -th position within the vehicle (pallets are numbered consecutively from the rear to the front of the vehicle), while \bar{r}_k is the time needed to drop off a unit in position k .

$$\bar{r}_k = \chi + 2\psi \times \lfloor \frac{k-1}{\epsilon} \rfloor \quad k = \{1, \dots, Q\} \tag{20}$$

Constraints (21) and (22) establish the relation between the r_{ij} and the main variables x_{ij} ; for the depot we fix $r_{00} = 1$.

$$\sum_k^Q r_{ik} = 1 \quad \forall i \in \mathcal{C} \tag{21}$$

$$x_{ij} \left(\sum_k^Q k(r_{jk} - r_{ik}) - q_i \right) = 0 \quad \forall (i, j) \in \mathcal{A} \tag{22}$$

Constraints (22) can be easily linearised as follows:

$$\sum_k^Q k(r_{jk} - r_{ik}) - q_i \geq -M(1 - x_{ij}) \quad \forall (i, j) \in \mathcal{A} \tag{23}$$

$$\sum_k^Q k(r_{jk} - r_{ik}) - q_i \leq M(1 - x_{ij}) \quad \forall (i, j) \in \mathcal{A} \tag{24}$$

Constraints (25) and (26) define the arrival times at depot and customer nodes: for the starting depot the tour conventionally begins at time \bar{t}_0 .

$$t_0 = \bar{t}_0 \tag{25}$$

$$t_i + s_i + \sum_{s \in S} d_{ij} \times \frac{z_{ij}^s}{v^s} - t_j \leq M(1 - x_{ij}) \quad \forall (i, j) \in \mathcal{A} \tag{26}$$

The arrival time variable t_i impose a unique route direction, thereby eliminating any sub-tours, consequently the classical sub-tour elimination constraints become redundant. Finally, the domains of the variables are:

$$\begin{aligned}
 x_{ij} &\in \{0,1\} & \forall (i,j) \in \mathcal{A} \\
 u_{ij} &\geq 0 & \forall (i,j) \in \mathcal{A} \\
 z_{ij}^s &\in \{0,1\} & \forall (i,j) \in \mathcal{A}, \forall s \in S \\
 w_{ij}^k &\in \{0,1\} & \forall (i,j) \in \mathcal{A}, \forall k \in K \\
 r_{ij} &\in \{0,1\} & \forall (i,j) \in \mathcal{A} \\
 t_i &\geq 0 & \forall i \in \mathcal{N} \\
 s_i &\geq 0 & \forall i \in \mathcal{N}
 \end{aligned}$$

It should be noticed that this formulation implicitly allows pre-service waiting times at customer nodes, i.e., the vehicle is allowed to wait idly at the customer node before starting to serve the customer. This is necessary to guarantee the “non-passing” (or FIFO) [33] property which requires that if a vehicle departs from node i to travel to node j , an earlier departure time produces an earlier arrival time, and vice versa.

Example

An exemplary instance with three customer nodes and a depot is shown in Figure 1, where the value reported on each arch refers to its length in km.

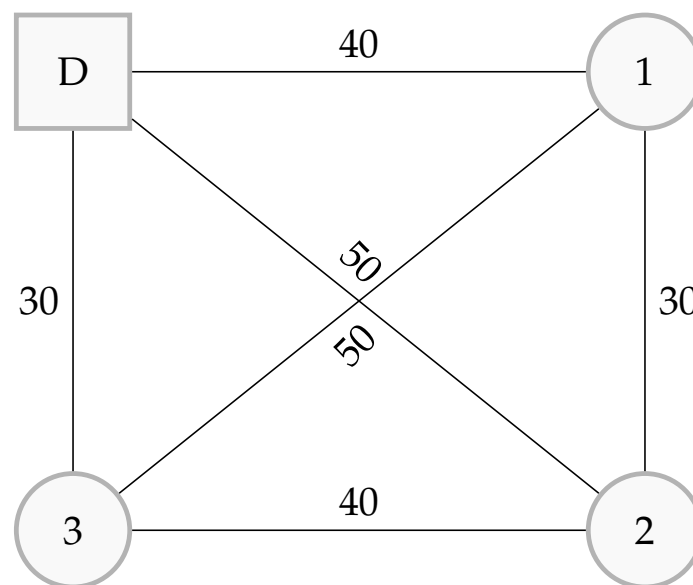


Figure 1. Example instance with 3 customers.

Figure 2 shows the independent decision variables of the mathematical model for the sample instance in Figure 1, i.e., the arcs x_{ij} that have to be included in the route and the arrival time t_i at each node. Conventionally, the depot has been duplicated into the starting depot (node 0) and the ending depot (node $n + 1$).

The mathematical model counts $(n^2 + n)$ independent binary variables x_{ij} , $(n + 2)$ independent integer-valued variables t_i , and $7n^2 + 15n + 11$ constraints, such that for this example instance with three customers and 24 speed and temperature time slots, the total number of independent variables is 12 and the number of constraints is 119.

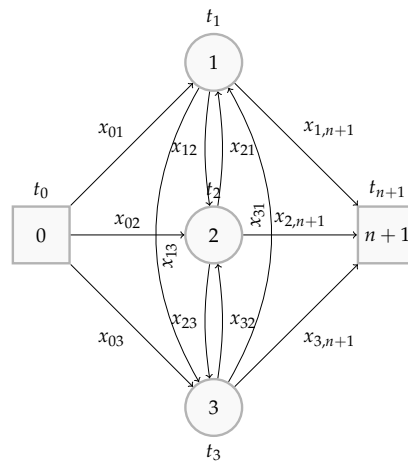


Figure 2. Independent decision variables of the mathematical model for the sample graph of Figure 1.

Figure 3a depicts the optimal route for the instance in Figure 1, as mapped in the graph of Figure 2 ($x_{03} = 1, x_{32} = 1, x_{21} = 1, x_{1,n+1} = 1, t_0 = 25,200, t_3 = 28,922, t_2 = 32,567, t_1 = 34,995, t_{n+1} = 38,880$).

We report on each arc the travel speed (in km/h). For each node, we show in brackets the pre-service waiting time (in seconds), the arrival time (hh:mm), and the service time (in seconds). We do not report data about temperature, because for the same time slots the outdoor temperature varies based on the month of the year.

In this example the vehicle departs from the depot at 7:00 a.m., and travels to node 3 for 30 km with a speed of 30 km/h. Before starting the service, the driver has to wait for 122 s, such that the actual arrival time is 8:02, and the unloading activity lasts 765 seconds. Then the vehicle leaves node 3 towards node 2, traveling for 40 km at 50 km/h. The pre-service waiting times for node 2 is null, such that the unloading service can start immediately at 9:02 and it takes 885 seconds. Subsequently, the vehicle moves to node 1, traveling for 30 km at 70/km; there is not waiting time and the vehicle arrives at 9:43, while the service time is equal to 1005. Finally, the vehicle goes back to the depot, which is 40 km far, traveling with a speed of 50 km, and it arrives there at 10:48.

Given the cost parameters reported on Table 1, the (yearly) total costs of this solution is $z = 45,066.7\text{€}$, whereas the detailed costs of the different components are: $F_{\text{trac}} = 30,814, F_{\text{trans}} = 2684.7, F_{\text{inf}} = 1666.4, F_{\text{driver}} = 9901.6$.

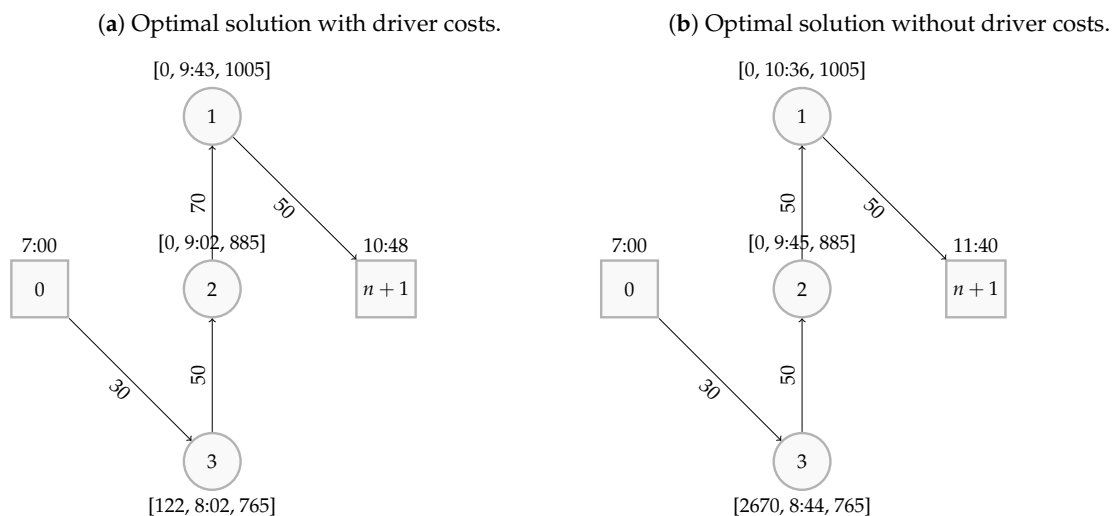


Figure 3. Optimal solutions for the example graph of Figure 1.

With the purpose to prove the importance of the driving cost component F_{driver} and its impact on the selection of the best solution, in Figure 3b it is reported the optimal route plan if F_{driver} is neglected. It can be noticed that the sequence of visited customers is the same as in Figure 3a, however arrival times, and consequently speed values and waiting times are different. In particular, it is request that the driver waits about 45 minutes at node 3 before starting unloading, so that all also the arrival time to the subsequent node is delayed of 43 min (9:45 instead of 9:02). The most evident implication is that arc (2, 1) is traversed with a speed of 50 km/h which is slower than the value of 70 km/h reported in the optimal solution of Figure 3a, with a consequent reduction of traction consumption of about 3% ($F_{\text{trac}} = 29,937.4$). Conversely, the consumption for refrigeration requirements is greater ($F_{\text{trans}} = 3289.7$, $F_{\text{inf}} = 1686.7$) given that the route duration is increased and the vehicle travels in hotter hours. The total cost (not considering the driver wage) is equal to 34,913.8€, compared to to 35,165.1€ of solution in Figure 3a.

4. Solution Methods

Our solution methods are based on a Constraint Programming model described in Section 4.1 and a local search technique presented in Section 4.2.

4.1. Constraint Programming Model

Analogously to [6], a Constraint Programming model is proposed for the problem, although from a different perspective. Indeed, in [6] the problem was formulated in a routing perspective as an extended VRP, that is the main decision variables are the arcs of the graph to be followed in the route visiting all the customers (see Figure 4). In this work, instead, similarly to the approach followed in [34] for a different logistics problem, a planning perspective is adopted. Indeed, in the case at hand, the route has to serve all the n customers and therefore the problem consists of determining a plan of $n + 2$ steps $s \in \{0, 1, \dots, n + 1\}$ where at each step the relevant decision variables are the customer to be served and the arrival times at that step (Figure 5). This planning perspective allows to avoid some of the constraints that were part of the routing model and were needed for maintaining a dual view on the operations at each customer, thus simplifying the model. Another feature of the proposed planning model is the possibility of arbitrarily long waiting times whereas the previous routing model used waiting times which were multiples of a specified time granularity (i.e., 5 min up to 30 min).

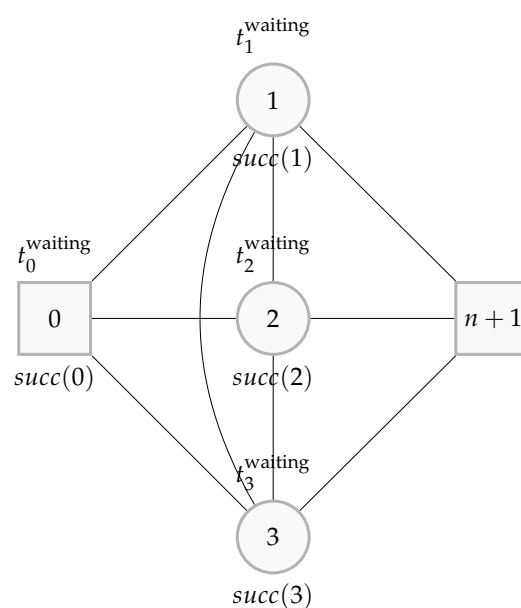


Figure 4. Independent decision variables of the CP model proposed in [6], where $succ(i)$ and t_i^{waiting} denote respectively the node successor of i and the time the vehicle waits at i .

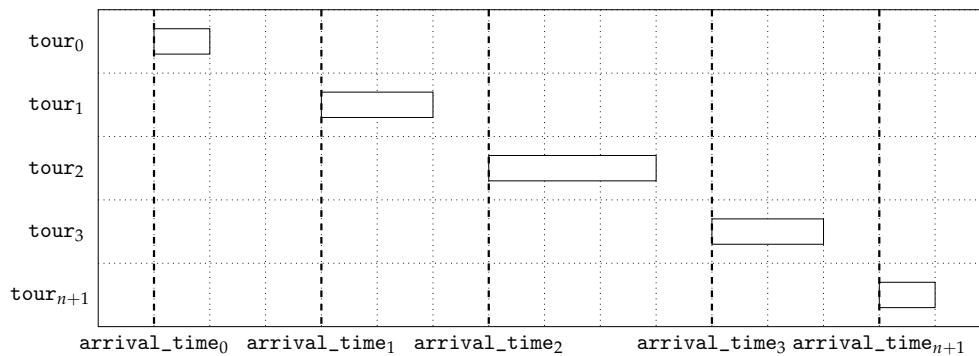


Figure 5. Independent decision variables of the new CP model, where tour_i and arrival_time_i denote respectively the node visited in the i -th step of the route plan and the corresponding arrival time.

In detail, more precisely, the Constraint Programming model consists of the following sets of variables and constraints.

The main decision variables $\text{tour}_s \in \{0, \dots, n+1\}$, for $s \in \{0, \dots, n+1\}$, specify who is the customer served at step s of the plan. The first step tour_0 is fixed to be the depot 0 so also the last step tour_{n+1} , for which the depot is $n+1$. The hamiltonian circuit property and sub-tour elimination is implicit in the model, just requiring that the values of the variables tour_s must be distinct, i.e.,:

$$\text{alldifferent}(\text{tour}) \quad (27)$$

The other set of integer decision variables $\text{arrival_time}_s \in \{0, \dots, 86,400\}$, for $s \in \{0, \dots, n\}$ determine the arrival time (measured in seconds) at the node served at step s . These variables do not simply functionally depend on the traveling times because of the possibility for the driver to wait before serving the customer.

Other time-related variables are processing_time_s , departure_time_s , and travel_time_s , $s \in \{0, \dots, n\}$, which account for the time needed to service the customer at step s and characterise the travel leaving the customer at step s and reaching the customer at step $s+1$. Notice that these variables are not needed for the last step of the plan (therefore they are just $n+1$ and not $n+2$). In the following, to simplify the notation, the index s will refer to the right set of values depending on the considered variables.

The latter time-related variables functionally depend on the setting of the decision variables. For example, processing_time_s depends on tour_s , the customer at step s , and the start_pallet_s the index of the first pallet to be discharged from the truck after all the customers $0, \dots, s-1$ have been served. Since this information can be computed beforehand, the possible processing times are stored in a matrix called unload_time_from logically indexed by these two information through an element constraint, i.e.,

$$\text{processing_time}_s = \text{unload_time_from}[\text{tour}_s, \text{start_pallet}_s] \quad (28)$$

Similarly, travel_time_s depends both on the customers served at step s and $s+1$ (actually their distance) and on the travel speed associated to the specific departure_time_s , therefore:

$$\text{travel_time}_s = \text{travel_speed}[\text{departure_time}_s / |K|] \cdot d[\text{tour}_s, \text{tour}_{s+1}] \quad (29)$$

Moreover, the departure time for the travel from step s to $s+1$ is determined as follows (departure_time_0 is set to the departure time from the depot):

$$\text{departure_time}_0 = \text{start_time_from_depot} \quad (30)$$

$$\text{departure_time}_s = \text{arrival_time}_s + \text{processing_time}_s \quad (31)$$

Finally, the relation for the $arrival_time_s$ variables is the following:

$$arrival_time_0 = departure_time_0 \quad (32)$$

$$arrival_time_{s+1} \geq departure_time_s + travel_time_s \quad (33)$$

Once the values of the time-related variables are set, the time-dependent cost function components (i.e., infiltration and transmission costs) can be expressed as formulae using lookups, using the `element` constraint, in some specific tables where the values are partially precomputed for a given temperature and month. For example, the transmission energy at step s (corresponding to Equation (14)) is determined as:

$$transm_consumption_s = \sum_{m \in M} transm_temp_s[temperature_slot_{sm}] \cdot (processing_time_s + travel_time_s) \quad (34)$$

The formula for the infiltration energy is similar to the one reported in Equation (15) in the MIP model.

As for the load-related variables, also those variables are determined in terms of the plan, for example the $vehicle_load_s$ and $start_pallet_s$ sets of variables are constrained as followed:

$$vehicle_load_0 = Q \quad (35)$$

$$vehicle_load_{s+1} = vehicle_load_s - q[tour_{s+1}] \quad (36)$$

and

$$start_pallet_0 = 0 \quad (37)$$

$$start_pallet_s = start_pallet_{s-1} - q[tour_{s-1}] \quad (38)$$

Analogously with the time-dependent cost components, also the load-dependent cost component is determined in a similar way as in the MIP model (Equation (3)).

The implemented model uses both `Int` and `Float` variables (these latter for the cost components) and extends `Gecode` with the implementation of the `element` constraint over arrays of `Float` values, which was not available in the system.

Finally, as the variable/value branching heuristics, from a set of preliminary experiments the best strategy has been determined as follows:

1. Branch on the `tour` variables, selecting the one having the maximum value for the Accumulated Failure Count and the values in increasing order;
2. Branch on the `arrival_time` variables, similarly selecting the one having the maximum value for the Accumulated Failure Count contribution and the values in increasing order;
3. Branch on the `cost_value` variable, splitting the domain in two halves around the median value (i.e., $\frac{\min + \max}{2}$).

Overall, the constraint programming model accounts for n decision variables $tour_s$, whose domain is $\{0, \dots, n\}$, and n decision variables $arrival_time_s$, whose domain is $\{0, 86, 400\}$.

The model is more succinct than the one used in an earlier work [6]. In particular, the use of the decision variables for the customers visits instead of the route successor variables of [6] (i.e., which is the next customer to be visited) allows to avoid the indirect indexing of the array of temporal CP variables (arrival/processing/waiting time) through the `element` constraint. The indirect reference would have required a considerable amount of constraint propagation at each solution search step which is avoided by the direct indexing of those variables (as in a regular array) in the new model.

Moreover, the novel model saves n decision variables (i.e., those accounting for the waiting times, which are implicitly modelled by using a set of departure times) and allows to express constraints

more naturally. Indeed, for a more precise comparison, the number of constraints involved in the two models is reported in Table 2, where only the relevant constraints are considered (i.e., equality constraints are disregarded). In particular, with respect to [6], the model is able to avoid many element constraints, thus considerably reducing the constraint propagation effort during the search.

Table 2. Comparison of the number of constraints in the CP model with respect to those of [6].

Global Constraints	New CP Model	CP Model [6]
alldifferent	1	1
circuit	—	1
sorted	—	1
element	$4(n - 1) + m \cdot (n - 1)$	$6(n - 1) + 7m(n - 1)$
Arithmetic constraints		
Inequality	$n - 1$	—

As for the example instance reported in Figure 1, with $n = 4$ nodes and $m = 24$ speed and temperature time slots, the total number of decision variables is 8 and the number of constraints is 88, whereas the routing CP model of [6] uses 12 decision variables and 525 constraints.

4.2. Local Search

In this section we outline the main problem-specific components of the local search algorithm employed in this study.

4.2.1. Search Space, Initial Solution and Cost Function

Looking at the mathematical and CP models defined in Sections 3 and 4.1, it could be noticed that the only independent decision variables are those related to the sequence of customers and the arrival times. Analogously, for the LS algorithm we choose a representation of a solution where a state in the search space is constituted only by two vectors of size n . The first one, similarly to the CP model, represents the permutation of nodes in the route, that is the order of customer to visit. The second one is a boolean-valued vector that states for each node $i \in \mathcal{C}$, if the vehicle has to wait at the node up to the start of the next speed time slot or not. Thereby, LS works on a reduced solution space whereas exact models consider any possible value for waiting times. The only practical reason for idle waiting at a node is to control the vehicle speed that depends on traffic congestion characterised by some peaks during the day, while temperature variations are smoother.

Adopting such solution representation gives the advantage that Constraints (4), (5) and (26) are automatically satisfied, thus always working with feasible solutions. Indeed, all the other constraints are only necessary to set the values of the dependent variables, which are used by the cost function.

The initial solution is a random permutation of the n nodes, without any waiting time. The cost function includes the cost components of the RRP defined in Equation (1), as detailed in Equations (2), (3) and (13).

4.2.2. Neighborhood Relations

The neighborhood used is a combination of two basic moves. The first one (called CN, for Change Node) changes the position of a node in a route, while the other one adds a waiting time to a node (WT, for Waiting Time). The waiting time for a node is computed as the difference between the start of the subsequent speed time slot and its current departure time. When a CN move is performed, all the waiting times of the nodes visited after the minimum between the old and the new position of the node, are set to 0. Given that the complete neighborhood used is the set union of the CN and WT basic relations, we use a probability to select first the neighborhood used, and then the specific move within the neighborhood (with uniform probability). In detail, WT is selected with probability p_{WT} and CN

with probability $1 - p_{WT}$. The value p_{WT} has been subject to tuning, along with the other parameters of the LAHC metaheuristic.

4.2.3. Late Acceptance Hill Climbing Metaheuristic

In order to guide the local search, we implemented the Late Acceptance Hill-Climbing (LAHC) algorithm has originally proposed by Burke and Bykov [35], which has been proven to be very effective in the context of routing problems.

At each step of the search, LAHC selects randomly one move from the neighborhood. The move is then accepted if the candidate solution improves or equals the cost function value of the solution which was the current several iterations before. As a consequence, the only control parameter is the length L_h of the list that records the previous values of the current cost function (history length).

As a stop criteria for LAHC, we used the number of iterations without improvement of the value of the cost function (stagnation detection), which has been set to 50,000 according to the results of preliminary experiments.

5. Results

The proposed model has been tested by referring to a basic scenario, which is described in details in the following Section 5.1. In Section 5.2, a comparative analysis of computational performance for the proposed solution methods is provided. Energy and cost performance of solutions for the reference scenario are analysed in Section 5.3. In Section 5.4, a more congested scenario is also analysed in order to derive the impact of a different speed profile on routes and waiting times. Sensitivity analysis has been performed on the time-dependent wage cost parameter and reported in Section 5.5.

Finally, different structures of the driver's wage cost are investigated in Section 5.6. Besides the cost proportional to the delivery process duration as in Equation (2), a fixed salary as well as a driver's payment proportional to the total travelled distance are considered, so that their impact on waiting times and sustainability performance achieved for the same delivery process can be derived.

5.1. The Reference Scenario

A parametrized instance generator has been developed in order to reproduce realistic data for different sizes of the delivery tour. The user specifies the desired number of nodes, the demand for each node, the vehicle parameters (see Table 1), the speed profile and the outdoor climate pattern. The position of each node is then randomly generated inside an area of $60 \times 60 \text{ km}^2$.

For the reference scenario, the average outdoor temperatures in hourly/monthly timeslots have been retrieved from the meteorological agency ARPA FVG OSMER, which collects the weather data for the Friuli-Venezia Giulia Region in North-Eastern Italy. As for the speed profile and travel distances, real data related to the investigated region have been collected from Google Maps. The resulting hourly speed values are reported in Table 3, describing the realistic traffic situations of a suburban area.

Table 3. Daily speed time slots for the basic scenario dataset D1.

Slot		Speed	Slot		Speed
Start	End	[km/h]	Start	End	[km/h]
00:00	06:00	70	13:00	14:00	45
06:00	07:00	60	14:00	15:00	50
07:00	08:00	40	15:00	16:00	55
08:00	09:00	45	16:00	17:00	50
09:00	10:00	50	17:00	18:00	45
10:00	11:00	50	18:00	19:00	40
11:00	12:00	45	19:00	20:00	50
12:00	13:00	40	20:00	24:00	60

We generated the dataset D1 of 14 test instances each with a number of nodes up to 17, and with a maximum total amount of palletized unit loads per delivery tour equal to the maximum vehicle capacity, which is 33 units for the adopted semi-trailer.

Indeed, this type of refrigerated transportation involves typically food delivered to supermarkets, thus the number of customers visited in a route is usually rather limited (see also [7]). Another restriction on the total number of nodes is given by the law regulation about the maximum number of consecutive driving hours, which in Italy is set to 9 h. However, in order to show how the different solution approaches scale on larger cases as reported in the following Section 5.2, we also generated an instance with 34 nodes (the maximum possible theoretical dimension for this scenario), which corresponds to 33 customers each having a demand of one unit, plus the depot.

For these instances, the demand is homogeneous, i.e., each node requires the same delivered quantity. Actually, cases with heterogeneous demand have been already investigated in [6], reaching the conclusion that customers with the larger demand are served at first, in order to obtain savings on the traction consumption related to the weight module of the CMEM model.

The name of each instance follows this pattern: Di-nj-npk, where *i* refers to the dataset, *j* is the number of nodes (depot included) and *k* is the total demand (palletized unit loads). All the instances employed in the paper and the best solutions obtained are available on the web for future inspection and comparison at <https://bitbucket.org/sceschia/the-refrigerated-routing-problem/>.

5.2. Computational Analysis

The results of the proposed solution techniques have been compared in terms of solution quality and computational times. For the MIP solver we use the default CPLEX configuration (v. 12.7.1). The CP model has been implemented in C++ using Gecode (v. 6.2.0) [36]. In addition we extended the CP model proposed in [6], which has been coded in MiniZinc (v. 2.0.14), by including also the driver cost. We ran CPLEX, Gecode and MiniZinc sequentially in deterministic mode, with a common time limit of one hour. The LAHC algorithm has been written in C++, using the EasyLocal++ framework [37], and compiled using the GNU C/C++ compiler (v. 4.4.3) under Ubuntu Linux. All experiments were run on an Intel® i7-7700 (3.60 GHz) machine.

The tuning phase for the LAHC metaheuristic has been performed using the tool JSON2RUN [38], which implements the F-Race procedure [39] (p -value = 0.02) for comparing the different parameter configurations. The resulting best configuration was: $p_{WT} = 0.1$ and $L_h = 25,000$.

The results for the RRP obtained by the different solution methods are shown on Table 4 and Figure 6. The LAHC metaheuristic was run 30 times on each instance, collecting the average, the best value and the running time. As for the MIP and the CP models, instead, only the results of a single run are reported, since they have no stochastic component. Proven optimal solutions are marked by * whereas best values are highlighted in bold; the dash symbol is used whenever the solver was not able to find any solution in the granted time.

From the results reported in Table 4, it can be noticed that LAHC is able to find all the proven optimal solutions (cases up to 12 nodes) and the best solutions for all the other cases; in addition the metaheuristic technique exhibits a high robustness given that average values are equal to minimum ones on 11 of 15 instances. For larger instances, the exact approaches are clearly outperformed by the LAHC in shorter computational times. In particular, for instance D1-n34-np33 they have not been able to find any feasible solution within one hour.

As for the comparison between the two CP models, the planning model proposed in this paper is able to consistently find solutions (although not optimal) for all problem sizes within the granted time bound. On the contrary, the routing model proposed in [6] scales up to 10 nodes but is not able to find any solution for bigger problem sizes in the allowed running time.

Table 4. Results on dataset D1: objective function values [€] and running times [s].

Instance	CP Routing [6]		CPLEX		CP Planning		LAHC		
	z	Time	z	Time	z	Time	Avg z	Min z	Time
D1-n4-np33	* 45,033.7	0.3	* 45,033.7	0.6	* 45,033.7	7.6	45,033.7	45,033.7	3.7
D1-n5-np32	* 37,771.5	0.9	* 37,771.5	1.8	* 37,771.5	2.2	37,771.5	37,771.5	3.8
D1-n6-np30	* 54,125.7	164	* 54,125.7	9.6	* 54,125.7	415	54,186.4	54,125.7	4.3
D1-n7-np30	* 45,605.8	193	* 45,605.8	63	* 45,605.8	17.8	45,605.8	45,605.8	4.7
D1-n8-np28	* 51,347.7	1516	* 51,347.7	117	* 51,347.7	94.9	51,347.7	51,347.7	5.6
D1-n9-np32	71,357.6	3600	43,591.1	3600	* 43,591.1	26.3	43,591.1	43,591.1	8.2
D1-n10-np27	78,744.8	3600	72,433.9	3600	* 66,982.9	364.6	67,114.6	66,982.9	9.7
D1-n11-np30	115,664.9	3600	71,620.9	3600	* 53,828.5	271.5	54,175.5	53,828.5	9.9
D1-n12-np33	109,173.7	3600	108,015.0	3600	* 59,091.2	1597.4	59,091.2	59,091.2	10.3
D1-n13-np24	124,985.2	3600	98,232.4	3600	56,692.2	3600	56,692.2	56,692.2	13.6
D1-n14-np26	140,885.5	3600	109,270.0	3600	95,558.0	3600	64,561.4	64,561.4	14.3
D1-n15-np28	148,593.2	3600	134,534.0	3600	75,444.8	3600	56,639.3	56,639.3	16.5
D1-n16-np30	169,970.0	3600	163,666.0	3600	119,894.0	3600	66,987.7	66,987.7	20.5
D1-n17-np32	165,214.5	3600	156,708.0	3600	102,083.0	3600	61,256.5	61,256.5	22.4
D1-n34-np33	–	–	–	–	–	–	100,906.6	98,228.5	67.4

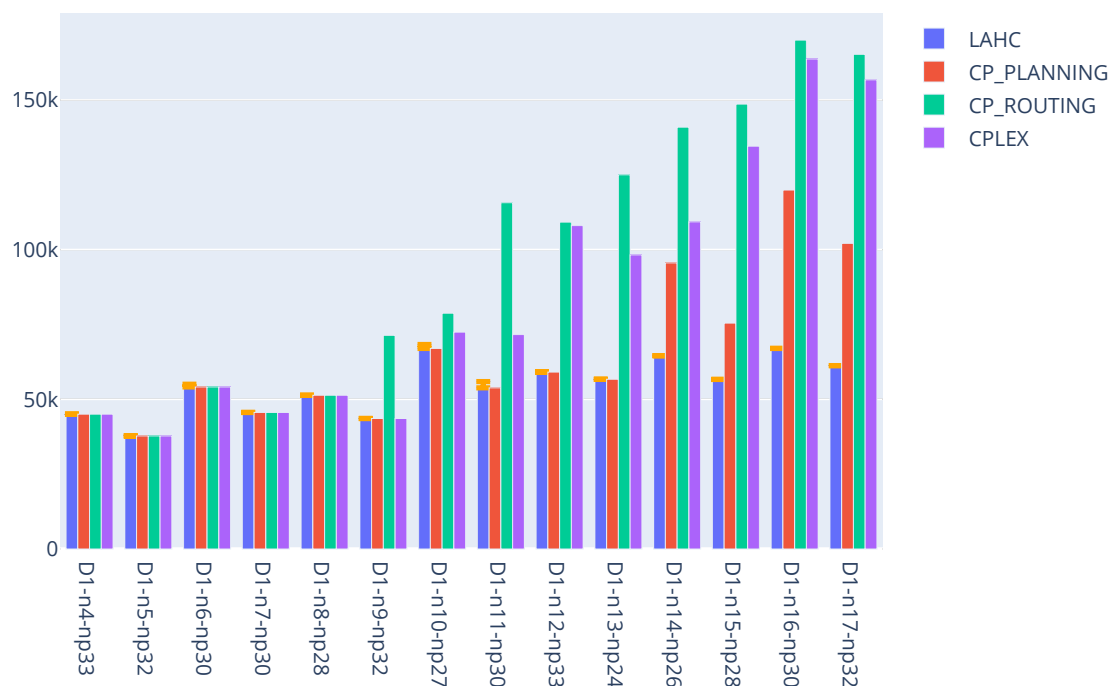
**Figure 6.** Comparative performance of different solution methods.

Figure 6 shows the performance of the different solution methods, grouped by instance (excluding instance D1-n34-np33, given that the only results available are those of LAHC). It is possible to notice that LAHC consistently outperforms the other approaches, exhibiting, in general, lower costs and a reasonably compact range of variation (shown by the orange deviation bars with respect to the average cost found by the method); indeed the other methods either find a solution with a considerably higher cost or are not able to find any feasible solution at all.

The main motivation for the poor performance of the exact methods is the complexity of the problem formulation, in particular Equations (14) and (15), that refer to the transmission and infiltration energy, introduce non linear terms, which are not naturally handled by the solvers.

All the best solutions but one (instance D1-n13-np24) are obtained without triggering waiting times at clients. This happens because waiting times usually increase the total tour duration, and consequently the driver wage which is a relevant part of the total cost. For the adopted speed profile this cannot be compensated by more favourable traffic or outdoor climate conditions. Specifically, a really short waiting time is convenient only for instance D1-n13-np24 just in the case of one customer. Indeed, because of the modeling characteristics, delaying the departure allowed the vehicle to travel at a greater speed (45 km/h with respect to 40 km/h without waiting). That reduces the travel time and consequently the transmission consumption and the driver wage, which are proportional to the tour duration.

5.4. Analysis of a Traffic-Congested Scenario

In this subsection, a traffic-congested scenario is taken into account by generating a dataset D2. With respect to the basic configuration analysed in the previous subsections, this scenario depicts the situation where there are fast and significant variations of the speed values also between adjacent timeslots, as typical for traffic congestion in rush hours (see Figure 8).

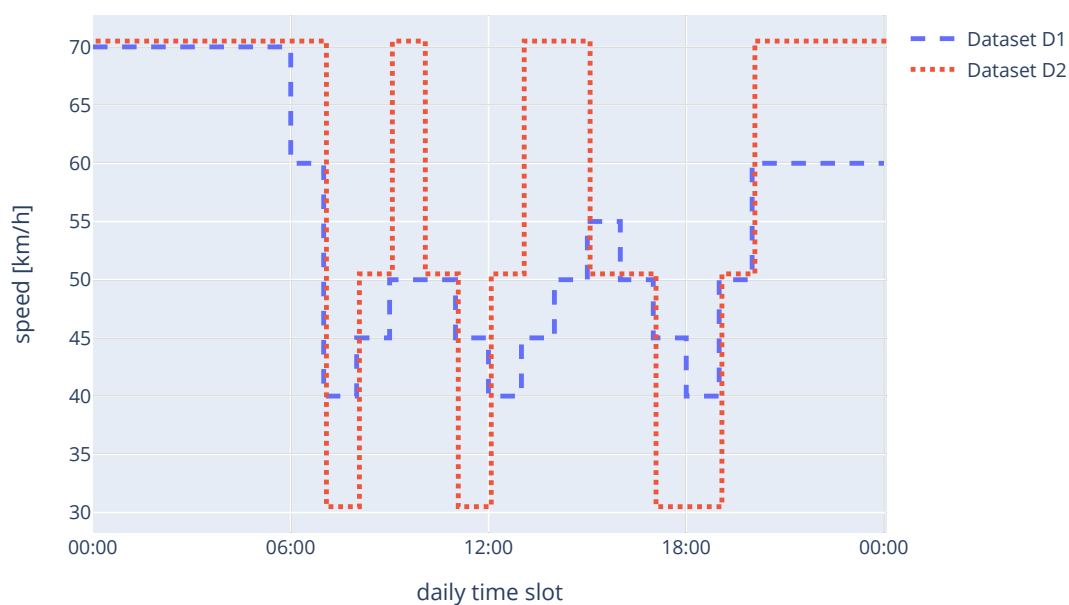


Figure 8. Daily speed time slots for the traffic-congested dataset D2 and its comparison with the reference scenario D1.

First of all, similarly to the previous analyses, we report in Table 6 the comparative results of the different solution methods on this dataset in the same setting employed in Section 5.2. Even for this dataset the results confirm that the LAHC method is the most effective one. In this case, however, on smaller instances some optimal solutions found by exact methods are beyond the reachability of LAHC (instances D2-n4-np33, D2-n5-np32, D2-n7-np30, Table 6), although the worst gap w.r.t. to the average values of LAHC is still within 1%.

Concerning the other solution methods, it should be noticed that on this dataset, the CP model proposed in [6] is not able to find the optimal solutions even for small cases since the domain of the waiting time variables is reduced to values ranging from 0 to 6, which represent time intervals of 5 min each (i.e., maximum 30 min). In addition, for instances with more than 10 nodes, it was not able to find any feasible solution within 1 h.

Table 6. Results on dataset D2: objective function values [€] and running times [s].

Instance	CP Routing [6]		CPLEX		CP Planning		LAHC		
	z	Time	z	Time	z	Time	Avg z	Min z	Time
D2-n4-np33	36,146.9	1.2	* 35,960.5	0.439	35,960.5	3600	36,063.6	35,980.6	4.1
D2-n5-np32	31,141.4	1.4	* 29,706.4	2.12	29,716.1	3600	29,716.5	29,707.7	5.2
D2-n6-np30	42,573.2	4.7	* 42,573.2	14.84	42,573.2	3600	42,573.2	42,573.2	4.3
D2-n7-np30	38,312.7	60	* 36,130.1	135	36,233.0	3600	36,190.3	36,138.5	8.9
D2-n8-np28	39,805.6	112	* 39,805.7	946	40,593.0	3600	39,968.3	39,805.7	5.8
D2-n9-np32	37,370.4	3600	33,439.5	3600	44,667.1	3600	33,480.6	33,450.7	10.9
D2-n10-np27	64,977.3	3600	54,517.2	3600	73,189.5	3600	52,986.5	52,779.5	12.3
D2-n11-np30	–	3600	45,305.4	3600	71,452.4	3600	42,600	42,147.9	15.7
D2-n12-np33	–	3600	75,671.5	3600	81,994.9	3600	46,248.1	46,221.1	16.4
D2-n13-np24	–	3600	81,188.4	3600	76,844.7	3600	44,156.3	44,118.4	20.2
D2-n14-np26	–	3600	87,372.7	3600	79,720.2	3600	49,790.9	49,778.6	25.2
D2-n15-np28	–	3600	79,524.3	3600	81,212.1	3600	43,838.1	43,800.1	24.5
D2-n16-np30	–	3600	73,351.4	3600	83,858.7	3600	52,053.0	51,926.4	31.4
D2-n17-np32	–	3600	89,769.6	3600	85,098.6	3600	47,016.5	46,985.5	36
D2-n34-np33	–	–	–	–	–	–	81,491.9	77,451.3	73.4

Moving to a specific analysis of the waiting times, results in Table 7a highlight how a more significant speed variation between adjacent time slots triggers waiting times in order to avoid traffic congestion and benefit from related faster travel times, which impact both on transmission energy requirements (see Equation (14)) and traction fuel consumption (as in Equation (3)). Due to wage cost minimisation, which is proportional to the delivery process duration, waiting times are limited to just the amount needed to activate a more convenient speed value. On the one hand, this underlines that modelling arbitrary waiting times as described in Section 3, instead of discrete waiting periods of 300 s each as in [6], allows to identify optimal driver’s behaviours. On the other hand, this suggests the opportunity to increase the accuracy of the model by also introducing the wage cost component to limit excessive stop times at clients.

The latter hypothesis is confirmed by the solutions obtained for the same dataset D2, when the wage cost is neglected (see Table 7b) and an upper bound on the overall delivery process duration is set to not exceed the maximum driving time imposed by law (e.g., 9 h for Italy). In comparison to the solutions reported in Table 7a, the same routes are obtained, but longer waiting times are selected in order to gain the most favourable speed values and reduce travel time consequently. The increased refrigeration requirements needed to counterbalance transmission load, which depend on the elapsed time the vehicle is exposed to outdoor temperature (see Equation (14)), cannot overcome, in facts, fuel savings for traction. Thus, if the driver wage cost component is neglected, more globally energy efficient behaviours are selected. For the analysed instances, the improvement on fuel consumption and therefore on related GHG emissions does not exceed 3%. Therefore, such a greener approach should be adopted basing on the goals to be pursued by the company in charge of the delivery process, which should manage potential driver and vehicle capacity underutilisation.

5.5. Sensitivity Analysis

To further investigate the role of the wage component, a sensitivity analysis on the related cost parameter f_d (see Equation (2) and Table 1) has been performed. For the reference case, solutions in terms of both route and waiting times remain unchanged for different f_d values.

Therefore, it can be derived that for a speed profile with slightly different values between adjacent time slots, waiting times are seldom convenient even for very low values of f_d . Table 7 suggests, instead, that for a more variable speed pattern as that of dataset D2, the wage cost parameter can play a more significant role.

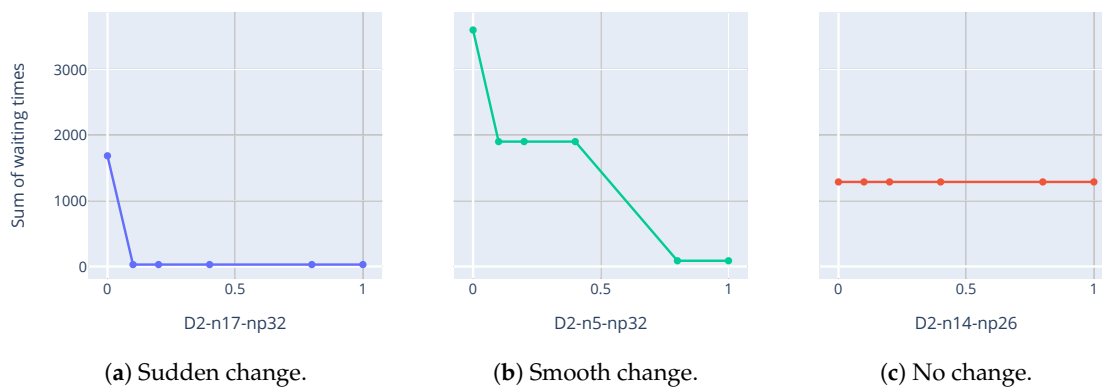


Figure 9. Sensitivity analysis on total waiting time per delivery route for different values of $f_d = \omega \cdot 7.92 \text{ €/h}$ on dataset D2, $\omega \in \{0.0, 0.1, 0.2, 0.4, 0.8, 1.0\}$. Representative instances for each of the three types of response are reported.

5.6. Modelling Different Wage Structures

The wage cost component for the extended RRP has been modelled, commonly to most routing literature, as proportional to the delivery process duration (see Equation (2)). The sensitivity analysis in the previous Section 5.5 has highlighted how, whenever the speed profile allows significant improvement of travel times, adding the wage to fuel consumption cost lead to control waiting times at clients.

To investigate whether a different cost structure can lead to different solutions, further experiments and analyses have been performed.

A fixed wage for the driver is equivalent to neglect the wage cost component from the objective function, since a constant cannot change the optimal route and related waiting times. Therefore, insights of the impact of this cost structure can be derived by analysing the time-dependent wage when f_d is set to a null value. As already observed by comparing Table 7, in this case the route doesn't change, but more waiting times are triggered to achieve the best overall fuel consumption along the whole delivery tour, without limits imposed by the need of not excessively prolonging the process due to the driver's wage. From an environmental point of view, as underlined in the previous Section 5.5, the solutions are related to lower fuel consumption and therefore lower GHG emissions, but they should be adopted by a company when energy efficiency is the primary goal and potential underutilisation of drivers and vehicles can be faced.

If a wage proportional to the travelled distance is taken into account, then Equation (2) should be replaced by the following Equation (39), where g_d is the cost per unit distance:

$$F_{\text{driver}} = g_d \times v \times \sum_{(i,j) \in \mathcal{A}} d_{ij} \times x_{ij} \quad [\text{€}] \quad (39)$$

Experiments on dataset D1 for g_d equal to 0.22 €/km have led to the same results in terms of route and waiting times obtained for the time dependent wage. As concerns instead dataset D2, where more significant speed value variations between adjacent time slots have been considered, this different wage structure leads to trigger waiting times greater than the time-dependent wage ones (see Table 8), but lower than the fixed wage values. Since distance affects not only the driver wage, but also the fuel consumption for traction, as shown in the CMEM model (Equation (3)), when it is introduced in another significant cost component of the objective function as in the distance-based wage, then its overall effect is reducing the weight of the time dependent cost component and potential benefits of later departures from clients consequently. As concerns the selected routes, they remain unchanged in comparison to the time-dependent and fixed wage circuits in 13 out of 15 cases. Analysing the two involved instances, the permutation of clients in the distance-based wage route allows to get both a

lower overall distance and greater speed values, which counterbalance the cost components affected by prolonged delivery duration due to waiting times.

Table 8. Values of the best solution of dataset D2 with driver wage cost proportional to the travelled distance: F [€], waiting times [s].

Instance	F_{trans}	F_{inf}	F_{trac}	F_{driver}	z	Waiting Times
D2-n4-np33	3294.3	1686.7	31,158.9	10,350.3	46,490.2	[0 315 1179 0]
D2-n5-np32	3221.5	1867.0	24,619.2	8902.7	38,610.4	[0 87 1680 1833 0]
D2-n6-np30	3257.8	2087.8	37,227.6	12,738.9	55,312.1	[0 0 0 0 0]
D2-n7-np30	3891.0	2336.4	29,911.1	10,639.9	46,778.4	[0 0 0 126 3015 0 534]
D2-n8-np28	3703.9	2537.8	33,564.0	12,304.6	52,110.3	[0 0 0 0 0 0 0]
D2-n9-np32	3055.2	2868.5	27,531.9	10,205.6	43,661.2	[0 0 3 0 0 0 0 491 0]
D2-n10-np27	4740.3	3132.3	44,906.9	16,213.1	68,992.6	[0 0 0 621 0 43 0 0 0 0]
D2-n11-np30	4385.9	3498.5	34,267.1	12,159.8	54,311.3	[0 0 327 837 0 1710 0 0 0 186 0]
D2-n12-np33	4069.7	3890.2	38,261.2	13,028.4	59,249.5	[0 288 0 0 0 0 0 79 0 0 0 0]
D2-n13-np24	4802.7	3928.2	35,392.5	13,317.9	57,441.3	[0 0 0 0 0 2904 0 0 0 231 126 0 0]
D2-n14-np26	4684.9	4166.3	40,934.5	15,344.6	65,130.3	[0 0 0 0 0 0 0 899 31 159 0 0 198 0]
D2-n15-np28	4653.2	4507.8	34,640.8	12,666.5	56,468.3	[0 0 0 483 0 0 0 2163 0 0 0 333 533 0 0]
D2-n16-np30	4909.3	4911.2	42,115.5	14,982.7	66,918.7	[0 0 0 0 0 0 0 766 0 0 0 579 246 0 0]
D2-n17-np32	4871.0	5222.0	36,893.4	13,317.9	60,304.3	[0 0 0 0 0 0 0 1660 25 0 0 0 0 0 0 0]
D2-n34-np33	8940.6	9375.2	57,978.7	19,759.7	96,054.2	[0 0 1320 0 0 0 2871 0 0 0 0 0 0 1764 0 0 0 0 2667 2708 0 0 0 0 0 0 0 0 0 0 0 0]

6. Conclusions

In this study, an extension and different solution methods are proposed for the Refrigerated Routing Problem (RRP) [6], a generalization of the Traveling Salesman Problem in which fuel consumption should be minimized.

Differently from the literature on the Pollution Routing Problem, a refrigerated vehicle is considered such that the fuel consumption depends on both traction and refrigeration requirements. For the refrigeration load, the transmission and the infiltration components are considered, which depend on outdoor climate conditions, so that a multi-period model is required to tackle different temperatures along a day and different seasons. Traction fuel requirements are modelled following the CMEM approach, dividing them into the weight, engine and speed modules and considering a multi-period speed profile to account for congestion. In our extension, arbitrary waiting times at clients are allowed, in order to delay departure whenever beneficial to gain more favourable traffic conditions. The driver wage is also added to refuelling cost as a main component of the objective function to be minimised.

For the extended RRP, a mathematical formulation and a new constraint programming model are proposed, together with simple but effective local search based metaheuristics, namely Late Acceptance Hill Climbing. We implemented a parametrised instance generator which uses real data about weather conditions and we tested our solution approaches on two datasets of instances up to 34 customers. To evaluate the performance of the LAHC algorithm, we compared it with exact methods that implement the MIP and CP models. The obtained results show that LAHC is able to derive the optimal or best solution on all instances in short computational time.

Comparison of different traffic scenarios has shown how the speed profile plays a major role on activating waiting time at clients, independently of the wage cost structure adopted. Departure delays, in facts, are triggered only for sensible variations in speed values between consecutive time slots, as typical of urbanised areas in rush hours. In this case, the time-dependent wage, which is the most adopted in literature, limits waiting times at clients, since benefits on traction fuel requirements are smoothed by driver cost increase. For a fixed wage cost policy, instead, waiting times grow in order to gain the best overall energy efficiency, since improvement on traction requirements exceeds worsening on refrigeration ones due to longer delivery durations. Finally, a wage cost based on travelled distance leads to balance the need of reducing the route length with the opportunity of delays at clients to avoid

traffic congestion, because of the impact on fuel consumption for traction, thus leading to intermediate behaviour in terms of delaying departures from clients.

Future work will be devoted to extend the problem formulation to the multi-vehicle case and develop hybrid approaches that integrates local search with CP or MIP techniques, in order to solve instances with a fleet of vehicles and a larger number of customers.

Author Contributions: Conceptualization, S.C., L.D.G. and A.M.; software, S.C., L.D.G. and A.M.; investigation, S.C., L.D.G. and A.M.; data curation, S.C., L.D.G. and A.M.; visualization, S.C., L.D.G. and A.M.; writing—review and editing, S.C., L.D.G. and A.M. All authors have read and agreed to the published version of the manuscript.

Funding: This research received no external funding.

Conflicts of Interest: The authors declare no conflict of interest.

References

1. Refrigerated Transport Market by Application (Chilled Food and Frozen Food), Mode of Transportation (Road, Sea, Rail, and Air), Vehicle Type (LCV, MHCV, and HCV), Temperature (Single and Multi-Temperature), Technology, and Region—Global Forecast to 2025; Technical Report; Refrigerated Transport Market, 2019. Available online: <https://www.marketsandmarkets.com/Market-Reports/refrigerated-transport-market-779494.html> (accessed on 15 July 2020).
2. Zhao, X.; Ke, Y.; Zuo, J.; Xiong, W.; Wu, P. Evaluation of sustainable transport research in 2000–2019. *J. Clean. Prod.* **2020**, *256*. [CrossRef]
3. Meneghetti, A.; Monti, L. Greening the food supply chain: An optimisation model for sustainable design of refrigerated automated warehouses. *Int. J. Prod. Res.* **2015**, *53*, 6567–6587. [CrossRef]
4. James, S.J.; Swain, M.J.; Brown, T.; Evans, J.A.; Tassou, S.A.; Ge, Y.T.; Eames, I.; Missenden, J.; Maidment, G.; Baglee, D. *Improving the Energy Efficiency of Food Refrigeration Operations*; Technical Report; The Institute of Refrigeration: London, UK, 2009.
5. Liu, G.; Hu, J.; Yang, Y.; Xia, S.; Lim, M.K. Vehicle routing problem in cold Chain logistics: A joint distribution model with carbon trading mechanisms. *Resour. Conserv. Recycl.* **2020**, *156*, 104715. [CrossRef]
6. Meneghetti, A.; Ceschia, S. Energy-efficient frozen food transports: The Refrigerated Routing Problem. *Int. J. Prod. Res.* **2019**. [CrossRef]
7. Stellingwerf, H.M.; Kanellopoulos, A.; van der Vorst, J.G.; Bloemhof, J.M. Reducing CO₂ emissions in temperature-controlled road transportation using the LDVRP model. *Transp. Res. Part D Transp. Environ.* **2018**, *58*, 80–93. [CrossRef]
8. Persyn, D.; Díaz-Lanchas, J.; Barbero, J. *Estimating Road Transport Costs Between EU Regions*; Technical Report JRC114409; European Commission Joint Research Center: Seville, Spain, 2019.
9. Demir, E.; Bektaş, T.; Laporte, G. A review of recent research on green road freight transportation. *Eur. J. Oper. Res.* **2014**, *237*, 775–793. [CrossRef]
10. Bektaş, T.; Laporte, G. The Pollution-Routing Problem. *Transp. Res. Part B Methodol.* **2011**, *45*, 1232–1250. [CrossRef]
11. Demir, E.; Bektaş, T.; Laporte, G. An adaptive large neighborhood search heuristic for the Pollution-Routing Problem. *Eur. J. Oper. Res.* **2012**, *223*, 346–359. [CrossRef]
12. Demir, E.; Bektaş, T.; Laporte, G. The bi-objective Pollution-Routing Problem. *Eur. J. Oper. Res.* **2014**, *232*, 464–478. [CrossRef]
13. Franceschetti, A.; Honhon, D.; Van Woensel, T.; Bektaş, T.; Laporte, G. The time-dependent pollution-routing problem. *Transp. Res. Part B Methodol.* **2013**, *56*, 265–293. [CrossRef]
14. Franceschetti, A.; Demir, E.; Honhon, D.; Van Woensel, T.; Laporte, G.; Stobbe, M. A metaheuristic for the time-dependent pollution-routing problem. *Eur. J. Oper. Res.* **2017**, *259*, 972–991. [CrossRef]
15. Ehmke, J.; Campbell, A.; Thomas, B. Vehicle routing to minimize time-dependent emissions in urban areas. *Eur. J. Oper. Res.* **2016**, *251*, 478–494. [CrossRef]
16. Ehmke, J.; Campbell, A.; Thomas, B. Optimizing for total costs in vehicle routing in urban areas. *Transp. Res. Part E Logist. Transp. Rev.* **2018**, *116*, 242–265. [CrossRef]
17. Xiao, Y.; Konak, A. The heterogeneous green vehicle routing and scheduling problem with time-varying traffic congestion. *Transp. Res. Part E Logist. Transp. Rev.* **2016**, *88*, 146–166. [CrossRef]

18. Xu, Z.; Elomri, A.; Pokharel, S.; Mutlu, F. A model for capacitated green vehicle routing problem with the time-varying vehicle speed and soft time windows. *Comput. Ind. Eng.* **2019**, *137*, 106011. [[CrossRef](#)]
19. Xiao, Y.; Zhao, Q.; Kaku, I.; Xu, Y. Development of a fuel consumption optimization model for the capacitated vehicle routing problem. *Comput. Oper. Res.* **2012**, *39*, 1419–1431. [[CrossRef](#)]
20. Koç, Ç.; Bektaş, T.; Jabali, O.; Laporte, G. The fleet size and mix pollution-routing problem. *Transp. Res. Part B Methodol.* **2014**, *70*, 239–254. [[CrossRef](#)]
21. De, A.; Kumar, S.K.; Gunasekaran, A.; Tiwari, M.K. Sustainable maritime inventory routing problem with time window constraints. *Eng. Appl. Artif. Intell.* **2017**, *61*, 77–95. [[CrossRef](#)]
22. De, A.; Wang, J.; Tiwari, M. Fuel Bunker Management Strategies Within Sustainable Container Shipping Operation Considering Disruption and Recovery Policies. *IEEE Trans. Eng. Manag.* **2019**. [[CrossRef](#)]
23. Zhang, G.; Habenicht, W.; Spieß, W. Improving the structure of deep frozen and chilled food chain with tabu search procedure. *J. Food Eng.* **2003**, *60*, 67–79. [[CrossRef](#)]
24. Rong, A.; Akkerman, R.; Grunow, M. An optimization approach for managing fresh food quality throughout the supply chain. *Int. J. Prod. Econ.* **2011**, *131*, 421–429. [[CrossRef](#)]
25. Zaroni, S.; Zavanella, L. Chilled or frozen? Decision strategies for sustainable food supply chains. *Int. J. Prod. Econ.* **2012**, *140*, 731–736. [[CrossRef](#)]
26. Aiello, G.; La Scalia, G.; Micale, R. Simulation analysis of cold chain performance based on time-temperature data. *Prod. Plan. Control* **2012**, *23*, 468–476. [[CrossRef](#)]
27. Accorsi, R.; Gallo, A.; Manzini, R. A climate driven decision-support model for the distribution of perishable products. *J. Clean. Prod.* **2017**, *165*, 917–929. [[CrossRef](#)]
28. Hsu, C.I.; Hung, S.F.; Li, H.C. Vehicle routing problem with time-windows for perishable food delivery. *J. Food Eng.* **2007**, *80*, 465–475. [[CrossRef](#)]
29. Novaes, A.; Lima, O.F., Jr.; De Carvalho, C.; Bez, E. Thermal performance of refrigerated vehicles in the distribution of perishable food. *Pesqui. Oper.* **2015**, *35*, 251–284. [[CrossRef](#)]
30. Nethercote, N.; Stuckey, P.J.; Becket, R.; Brand, S.; Duck, G.J.; Tack, G. MiniZinc: Towards A Standard CP Modelling Language. In *International Conference on Principles and Practice of Constraint Programming (CP 2007)*; Springer: Berlin/Heidelberg, Germany, 2007; pp. 529–543.
31. Barth, M.; Scora, G.; Younglove, T. Modal emissions model for heavy-duty diesel vehicles. *Transp. Res. Rec.* **2004**, *1*, 10–20. [[CrossRef](#)]
32. Lafaye De Micheaux, T.; Ducoulombier, M.; Moureh, J.; Sartre, V.; Bonjour, J. Experimental and numerical investigation of the infiltration heat load during the opening of a refrigerated truck body. *Int. J. Refrig.* **2015**, *54*, 170–189. [[CrossRef](#)]
33. Kuo, Y. Using simulated annealing to minimize fuel consumption for the time-dependent vehicle routing problem. *Comput. Ind. Eng.* **2010**, *59*, 157–165. [[CrossRef](#)]
34. Di Gaspero, L.; Rendl, A.; Urli, T. Balancing Bike Sharing Systems with Constraint Programming. *Constraints* **2016**, *21*, 318–348. [[CrossRef](#)]
35. Burke, E.K.; Bykov, Y. The late acceptance Hill-Climbing heuristic. *Eur. J. Oper. Res.* **2017**, *258*, 70–78. [[CrossRef](#)]
36. Schulte, C.; Tack, G.; Lagerkvist, M.Z. *Modeling and Programming with Gecode*; Corresponds to Gecode 6.2.0; 2019. Available online: <https://www.gecode.org/doc-latest/MPG.pdf> (accessed on 15 July 2020).
37. Di Gaspero, L.; Schaerf, A. EASYLOCAL++: An object-oriented framework for flexible design of local search algorithms. *Softw. Exp.* **2003**, *33*, 733–765. [[CrossRef](#)]
38. Urli, T. json2run: A tool for experiment design & analysis. *arXiv* **2013**, arXiv:1305.1112.
39. Birattari, M.; Yuan, Z.; Balaprakash, P.; Stützle, T. F-race and iterated F-race: An overview. In *Experimental Methods for the Analysis of Optimization Algorithms*; Springer: Berlin, Germany, 2010; pp. 311–336.

Publisher’s Note: MDPI stays neutral with regard to jurisdictional claims in published maps and institutional affiliations.



© 2020 by the authors. Licensee MDPI, Basel, Switzerland. This article is an open access article distributed under the terms and conditions of the Creative Commons Attribution (CC BY) license (<http://creativecommons.org/licenses/by/4.0/>).